

the factors D_0 , provide a simple parametrization to account for the absolute two-nucleon differential cross sections. Nonetheless, they were ~~can~~ a source of misunderstanding concerning the reaction mechanism of two-nucleon transfer, let alone of the spatial structure of Cooper pairs.

190

CHAPTER 3. SIMULTANEOUS VERSUS SUCCESSIVE TRANSFER

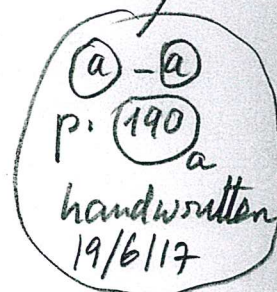
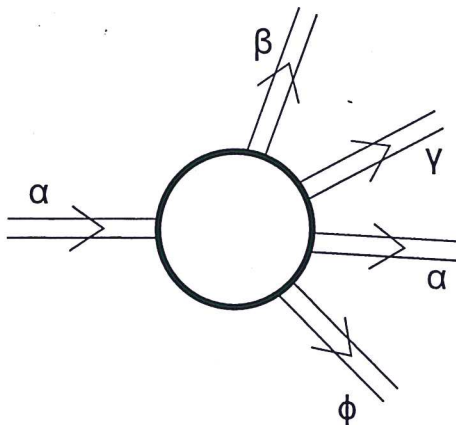


Figure 3.5.1: Schematic representation of entrance (α) and exit channels ($\beta, \gamma, \alpha, \phi$) of a nuclear reaction and of the interaction region.

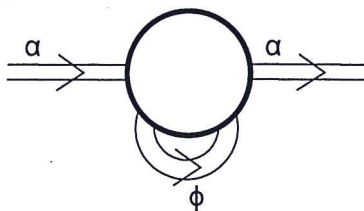


Figure 3.5.2: Schematic representation of the change in role of the one-nucleon transfer channel ϕ from being an open channel, (Fig. 3.5.1) to one which acts as a virtual channel contributing to the optical potential.

transfer process than those associated with $n = 1$ and 2 , that is those proportional to Ω_1 and Ω_2 whose values are 0.25 and 0.06 respectively (cf. Eq. (2.1.3)). All these features boost the effective absolute two-nucleon ~~pure configuration~~ transfer cross section to the observed experimental value. While the results displayed in Fig. 3.4.4 were calculated making use of the full formalism of second order DWBA (cf. Figs. 3.1.1 and 3.1.2) the simplified expressions given in Eqs. (2.1.1–2.1.7) are useful to gain physical insight into the two-nucleon transfer process. ~~form factors~~
 $U_{L_{Sf}}^{J_f J_f}(R)$. In fact, these functions, multiplied by 1

3.5 Comments on the optical potential

As a rule, the depopulation of the entrance, elastic channel $\alpha(a, A)$ (see Fig. 3.5.1) is mainly due to one-particle transfer channels $\phi(f = a - 1, F = A + 1)$. Other channels, like e.g. inelastic ones $\beta(a^*, A)$, $\gamma(a, A^*)$ being operative in particular situations, for example, when deformed nuclei are involved in the reaction process. Let us assume that this is not the case. Thus, quite likely, the one-particle transfer channel ϕ is expected to be the main depopulating channel of the entrance channel

① Let us elaborate on this point, making use of an analogy. Collective surface vibrations of closed shell nuclei can be viewed as correlated particle-hole excitations. The phase coherence existing between the different RPA amplitudes of the corresponding wave function leads to a decrease of the average distance between the particle and the hole, as compared with pure ph-configurations, similar to what happens in pair addition (subtraction) modes. In this case are the $p\bar{p}$ ($h\bar{h}$) which approach each other. It has been argued that this is the reason why both pairing and surface vibrations of closed shell nuclei display enhanced (t,p) cross sections as compared to pure configurations^{*)}. The two neutrons lie rather close to each other in the triton. (like e.g. the octupole vibration of ^{208}Pb ($E_x = 2.65 \text{ MeV}$),

Now, in the case of collective surface vibrations of closed shell nuclei, the specific probe is not two-nucleon transfer, but Coulomb excitation or inelastic scattering, and the corresponding γ -decay process. The wavelength associated with this γ -ray is $\lambda \approx 460 \text{ fm}$. Whether the probe particle lies closer or less to its correlated hole into which it has to fall in the decay process can, in any way, be related to the enhancement of the absolute transition probability ($B(E3) = 32 B_{sp}$) of a probe of wavelength almost two orders of magnitude larger than nuclear dimensions, is hard to understand. Not only this, it sets a question mark on the validity of the argument as applied to Cooper pair transfer and pairing correlations. This question is taken up in Sect. 3.8 and Apps. 3A - 3D. ①

^{*)} Bertsch et al (1967).

α (cf. Fig. 3.5.2). This is also in keeping with the fact that the tail of the corresponding form factors, reaches further away than that of any other channel (cf. Fig. 3.5.5). In this case, the calculation of the optical potential²⁶, is quite reminiscent to the calculation of two-particle transfer (2nd order process), and can be carried out with essentially the same tools. In fact,

$$\begin{aligned} T_{succ}^{(2)} &\sim \langle fin|v|int\rangle\langle int|v|in\rangle \\ T_{NO}^{(2)} &\sim \langle fin|v|int\rangle\langle int|\mathbf{1}|in\rangle, \end{aligned} \quad (3.5.1)$$

where $|in\rangle = |a, A\rangle$, $|int\rangle = |f, F\rangle$ and $|fin\rangle = |b, B\rangle$ are the initial, intermediate, and final channels in a two-nucleon transfer reactions, which become

$$\begin{aligned} \langle in|v|int\rangle\langle int|v|in\rangle \\ \langle in|v|int\rangle\langle int|\mathbf{1}|in\rangle, \end{aligned} \quad (3.5.2)$$

as contributions to the optical potential (Fig. 3.5.2).

Let us elaborate on the above arguments within the context, for concreteness, of ^{11}Li and of the reaction $^{11}\text{Li}(p, t)^9\text{Li}$. In keeping with the fact that structure and reactions are just but two aspects of the same physics and that in the study of light halo nuclei, continuum states are to be treated on, essentially, equal footing in the calculation of the wavefunctions describing bound states (structure) as well as of the asymptotic distorted waves entering in the calculation of the absolute two-particle transfer differential cross sections (reaction; see Figs. 3.5.3 (a) and (b)), the calculation of the optical potentials is essentially within reach (reaction, see Figs. 3.5.3 (c) and 3.5.4). Because the real and imaginary parts of complex functions are related by simple dispersion relations²⁷, it is sufficient to calculate only one of the two (real or imaginary) components of the self-energy function to obtain the full scattering, complex, nuclear dielectric function (optical potentials). Now, absorption is controlled by on-the-energy-shell contributions. Within this scenario it is likely that the simplest way to proceed is that of calculating the absorptive

complex
self energy
contribution
to the

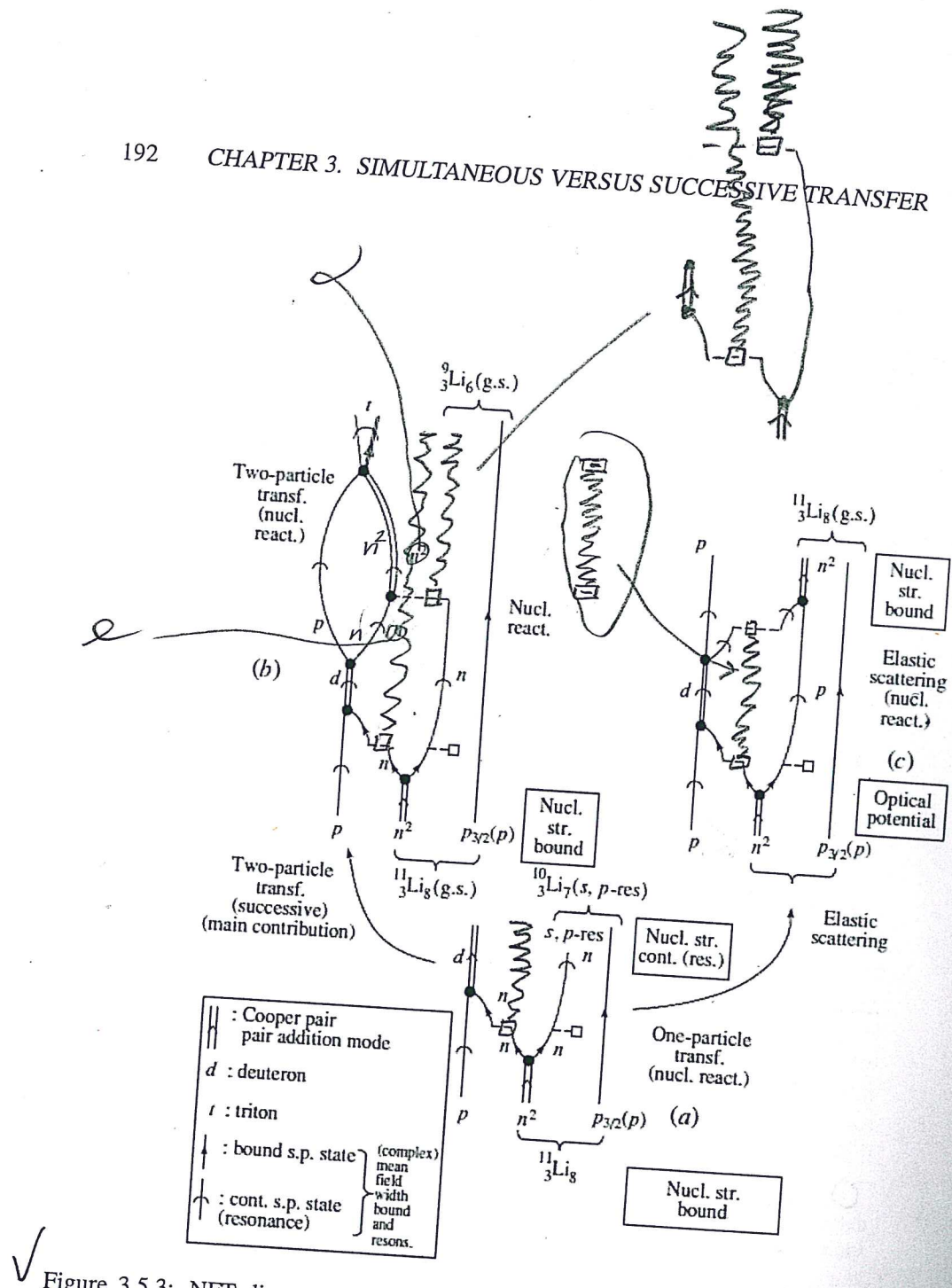
²⁶It is of notice that the optical potential can be viewed as the complex “dielectric” function of direct nuclear reactions. In other words, the function describing the properties of the medium in which incoming and outgoing distorted waves propagate, properties which are, as a rule determined through the analysis of elastic scattering processes, under the assumption that the coupling between the relative motion (reaction) and intrinsic (structure) coordinates, occur only through a Galilean transformation (recoil effect) which smoothly matches the incoming with the outgoing waves (trajectories). Now, within the present context, namely that of the microscopic calculation of $\bar{U} + iW$, non-locality and ω -dependence can be microscopically treated on equal footing through the calculation of structure properties. In particular, within the framework of NFT, taking into account the variety of correlations and couplings between single-particle and collective motion, elementary modes of nuclear excitation. Such an approach to structure and reaction provides the elements and rules for an *ab initio* calculations of the texture of the corresponding vacuum states, and thus of the bound and continuum properties of the nuclear quantal system by itself and in interaction. It is of notice that such a scenario includes also limiting situations like sub-barrier fusion processes (cf. e.g. Sargsyan, V. V. et al. (2013) and refs. therein) and also exotic decay (cf. e.g. Barranco, F. et al. (1988, 1990); Montanari et al. (2014), cf. also Brink, D. and Broglia (2005)).

²⁷See, e.g., Mahaux, C. et al. (1985) and references therein; Dikhoff, W. and Van Neek (2005).

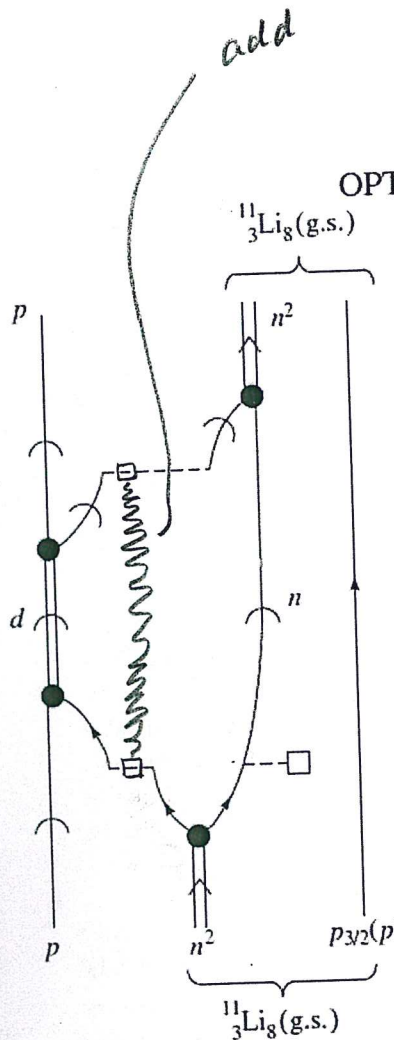
$\Delta E + iW$ (Fig. 3.5.4)

of polarization
and correlation
(self energy)
contributions
to the optical
potential, arising
from

↑
add list refs.



✓ Figure 3.5.3: NFT diagrams summarizing the physics which is at the basis of the structure of ^{11}Li (Barranco, F. et al. (2001)) and of the analysis of the $^{11}\text{Li}(p, t)^9\text{Li}(\text{g.s.})$ reaction (Potel et al. (2010)). In the figure emphasis is set on intermediate (like, e.g., $^{10}\text{Li} + d$, see (a) and (b)) and elastic (see (c), see also Fig. 3.5.4) channels.



$$\sum_p(k, \omega) = \sum_{\text{int}} \frac{V_{p, \text{int}}^2}{\hbar\omega - E_{\text{int}}},$$

$$= \lim_{\Delta \rightarrow 0} \sum_{\text{int}} \frac{V_{p, \text{int}}^2}{(\hbar\omega - E_{\text{int}}) + i\Delta/2},$$

$$= \Delta E_p(k, \omega) - iW_p(k, \omega),$$

$$\Delta E_p(k, \omega) = \lim_{\Delta \rightarrow 0} \sum_{\text{int}} \frac{(\hbar\omega - E_{\text{int}}) V_{p, \text{int}}^2}{(\hbar\omega - E_{\text{int}})^2 + \left(\frac{\Delta}{2}\right)^2},$$

$$W_p(k, \omega) = \lim_{\Delta \rightarrow 0} \sum_{\text{int}} \frac{\frac{\Delta}{2} V_{p, \text{int}}^2}{(\hbar\omega - E_{\text{int}})^2 + \left(\frac{\Delta}{2}\right)^2},$$

$$\Delta E_p(k, \omega) = U_p(k, \omega) = \frac{\mathcal{P}}{\pi} \int \frac{W_p(k, \omega)}{\omega - \omega'} d\omega'.$$

Kramers-Krönig

✓ Figure 3.5.4: NFT diagrams and summary of the expression (see, e.g., Mahaux, C. et al. (1985) and references therein) entering the calculation of one of the contributions (that associated with one-particle transfer and, arguably, the dominant one) to the ${}^{11}\text{Li} + p$ elastic channel optical potential. The self-energy function is one to the ${}^{11}\text{Li} + p$ elastic channel optical potential. The self-energy function is denoted Σ_p , while the real and imaginary parts are denoted $\Delta E_p (= U_p)$ and W_p , respectively, the subindex p indicating the incoming proton. These quantities are, in principle, functions of frequency and momentum.

potential and then obtain the real part by dispersion. Of notice that in heavy-ion reactions, one is dealing with leptodermous systems. Thus, the real part of the optical potential can, in principle, be obtained by convolution of the nuclear densities and of the surface tension⁽²⁸⁾. Within the present context, one can mention the ambiguities encountered in trying to properly define a parentage coefficient relating the system of $(A + 1)$ nucleons to the system of A nucleons, and thus a spectroscopic amplitude. In other words, a prefactor which allows to express the absolute one-particle transfer differential cross section in terms of the elastic cross section. Making use of NFT diagrams like the one shown in Fig. 3.5.4, it is possible to calculate, one at a time, the variety of contributions leading to one- and two-particle transfer processes as well as of the associated optical potential. Summing up the different contributions, taking also proper care of those arising from four-point vertex, tadpole processes, etc., a consistent description of the different channels can be worked out, in which the predicted quantities to be directly compared with observables are absolute differential cross sections, or, more generally, absolute values of strength functions for different scattering angles.

3.6 Weak link between superconductors

Two-nucleon transfer reactions involving superfluid nuclei display some similarities with Cooper pair tunneling between weakly coupled superconductors, in particular when discussing heavy ion reactions, but not only⁽²⁹⁾. Within this context it is useful to remind the basic elements of the pair tunneling which is at the basis of the Josephson effect. In this section we essentially reproduce the description of the tunneling of Cooper pairs between two weakly coupled superconductors to be found in⁽³⁰⁾, arguably, the best physical presentation of the Josephson effect⁽³¹⁾.

One starts with the many-body Hamiltonian of⁽³²⁾

$$H = H_1 + H_2 + \sum_{kq} T_{kq} (a_{k\uparrow}^\dagger a_{k\uparrow} + a_{-q\downarrow}^\dagger a_{-q\downarrow}) + HC \quad (3.6.1)$$

where H_1 and H_2 are the separate Hamiltonians of the two superconductors on each side of the barrier, T_{kq} being the (exponentially) small tunneling matrix element from state k on one side to q on the other.

One can arrive to (3.6.1) by first finding sets of single-particle wavefunctions for each side separately, in the absence of the potential of the other system. Then one eliminates the non-orthogonality effects by perturbation theory (cf. the similarity with the arguments used in Sect. 3.2 as well as Sect. 5.C; for details see Sect. 5.1). It is of notice that a nuclear embodiment of such strategy but for the

⁽²⁸⁾Cf. e.g. Broglia and Winther (2005) and references therein.

⁽²⁹⁾von Oertzen and Vitturi (2001); von Oertzen, W. (2013); Broglia and Winther (2004).

⁽³⁰⁾Anderson (1964).

⁽³¹⁾Josephson (1962).

⁽³²⁾Cohen et al. (1962).

app.

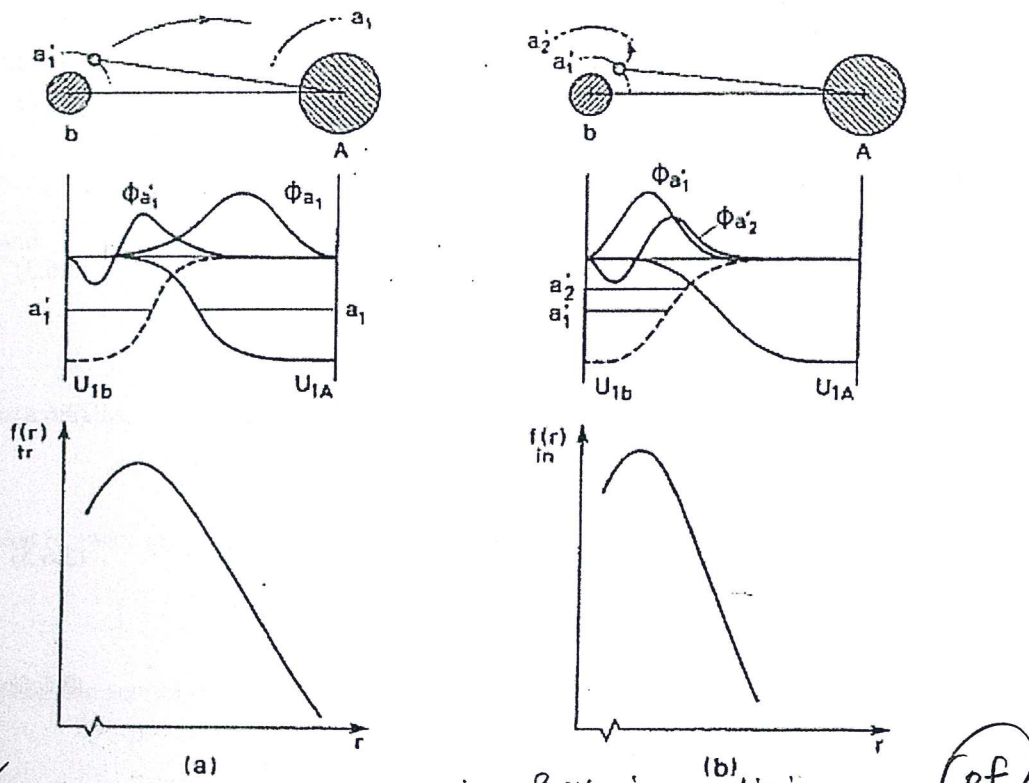


Figure 3.5.5: Schematic representation of the radial dependence of the one-particle transfer and inelastic form factors. In (a) a nucleon moving in the orbital with quantum numbers a'_1 in the projectile a is transferred under the action of the shell model potential U_{1A} to the target nucleus A into an orbital a_1 . The dependence of the form factor on the distance between the two nuclei is determined by the overlap of the product of the single-particle wavefunctions $\phi_{a'_1}$ and ϕ_{a_1} with the potential U_{1A} . A schematic representation of this dependence is given at the bottom of (a). In (b) a nucleon in the projectile a is excited under the influence of the target field U_{1A} from the single-particle orbital with quantum numbers a'_1 to the orbital with quantum numbers a'_2 . The dependence of the form factor on the distance between the cores is here determined by the overlap of the product of the functions $\phi_{a'_1}$ and $\phi_{a'_2}$ with the potential U_{1A} . A representation of this dependence is shown at the bottom of (b) (after Broglia and Winther (2005)).

It is of notice that at the basis of the Josephson effect one finds $P_2 \approx P_1$, which, in the nuclear case implies $\Omega_{\text{ap}} \approx \Omega_{\text{ip}}$. A remarkable finding whether both or a single interacting systems is a superfluid nucleus.

196 CHAPTER 3. SIMULTANEOUS VERSUS SUCCESSIVE TRANSFER

case superfluid-normal³³ tunneling is worked out in Ch. 5 and implemented in COOPER³⁴.

Let us now calculate the second order expression of (3.6.1) in the case in which the gaps of the two weakly linked superconductors are different. Making use of relations presented in Sect. 2.4.2 one can write, for $T = 0$,

$$\Delta E_2 = -2 \sum_{kq} |T_{kq}|^2 \frac{|V_k U_q + V_q U_k|^2}{E_k + E_q}. \quad (3.6.2)$$

With the help of

$$2U_k V_k^* = \frac{\Delta_k}{E_k}, \quad 2U_q V_q^* = \frac{\Delta_q}{E_q}, \quad (3.6.3)$$

and

$$|U_k|^2 - |V_k|^2 = \frac{\epsilon_k}{E_k}, \quad |U_q|^2 - |V_q|^2 = \frac{\epsilon_q}{E_q}, \quad (3.6.4)$$

where

$$E = \sqrt{\epsilon^2 + \Delta^2} \quad (3.6.5)$$

and

$$\Delta_k = \Delta_1 e^{i\phi_1}, \quad \Delta_q = \Delta_2 e^{i\phi_2} \quad (3.6.6)$$

one can write for the numerator of Eq. (3.6.2),

$$\begin{aligned} \text{NUM} &= (V_k U_q + V_q U_k)(V_k^* U_q^* + V_q^* U_k^*) \\ &= \{V_k^2 U_q^2 + V_q^2 U_k^2\} + [(U_k^* V_k)(U_q V_q^*) + (U_q^* V_q)(U_k V_k^*)]. \end{aligned} \quad (3.6.7)$$

It is of notice that, for simplicity, throughout this Appendix

$$V^2 \equiv |V|^2. \quad (3.6.8)$$

³³ It is of notice that pairing vibrations in nuclei are quite collective, leading to effective U and V occupation factor (cf. Fig. 3.3.2) (see also Potel, G. et al. (2013b)), the nuclear and the condensed matter expressions are very similar. Of course no supercurrent is expected between nuclei. However, the systems ¹²⁰Sn(gs), ¹¹⁹Sn(j), ¹¹⁸Sn(gs) form an ensemble of weakly coupled Fermi superfluids, with different (average) number of particles ($N, N - 1, N - 2$), to which essentially all the BCS techniques, including those of the present Appendix can be applied (cf. Fig. 3.7.1). Of notice the parallel of this scenario with that associated with nuclei excited at rather high energies for which one defines a temperature. This is possible, because the excited (thermalized) nucleus is in equilibrium with the particles, namely neutrons and gamma-rays it emits, particles which act as a thermal bath, let alone the very high density of levels, of the compound nucleus (cf. Bertsch and Broglia (2005) p 17).

³⁴ Cf. App. 6.D; cf. also Broglia and Winther (2005).

Bortignon et al (1998) p.7

It is of
intrinsic excitation

(A) - (A) pp. ①, ②, ③ handwritten
 labeled also 198_a 198_b 198_c Milano 21/6/17

where N_1 and N_2 are the density of levels of one spin at the Fermi energy one finally obtains

$$\begin{aligned}\Delta E_2 &\approx -N_1 N_2 \Delta_1 \Delta_2 \langle |T_{kq}|^2 \rangle \cos(\phi_1 - \phi_2) \int_{-\infty}^{\infty} \int_{-\infty}^{\infty} \frac{d\epsilon_1 d\epsilon_2}{E_1 E_2 (E_1 + E_2)} \\ &\approx -N_1 N_2 \langle |T_{kq}|^2 \rangle \cos(\phi_1 - \phi_2) 2\pi^2 \frac{\Delta_1 \Delta_2}{\Delta_1 + \Delta_2}\end{aligned}\quad (3.6.19)$$

Consequently, the maximum possible supercurrent is the same as the normal current at a voltage V_{equil} equal to $\pi \Delta_1 \Delta_2 / (\Delta_1 + \Delta_2)$.

3.7 Phase coherence

The phase of a wavefunction and the number of nucleons (electrons in condensed matter) are conjugate variables: gauge invariance, i.e. invariance under phase changes, implies number conservation in the same way that rotational invariance implies angular momentum conservation.

Example:

$$\Psi = a_1^\dagger a_2^\dagger \cdots a_N^\dagger \Psi_{\text{vac}}.$$

Multiplying the creation operators by a phase factor,

$$a'^\dagger = e^{-i\phi} a^\dagger,$$

one can rewrite

$$\begin{aligned}\Psi &= (e^{i\phi} a'_1^\dagger) (e^{i\phi} a'_2^\dagger) \cdots (e^{i\phi} a'_N^\dagger) \Psi_{\text{vac}} \\ &= e^{iN\phi} \Psi'.\end{aligned}$$

Thus

$$-i \frac{\partial}{\partial \phi} \Psi = N e^{iN\phi} \Psi' = N \Psi$$

where

$$N = -i \frac{\partial}{\partial \phi}; \quad \phi = i \frac{\partial}{\partial N}$$

and

$$[\phi, N] = 1; \quad \Delta\phi \Delta N = 1.$$

In this case Ψ (wavefunction referred to the laboratory system) and Ψ' (wavefunction referred to the intrinsic system) represent the same state. A phase change for a gauge invariant function is just a trivial operation. Like to rotate a rotational invariant function. Quantum mechanically nothing happens rotating a spherical system (in 3D-, gauge, etc.) space.

(A)

at an equivalent voltage^{*)}

198 ~

(1)

$$V_{\text{equiv}} = \frac{\pi \Delta_1 \Delta_2}{\Delta_1 + \Delta_2}, \quad (3.6.20)$$

For two identical superconductors

 $V_{\text{equiv}} = \frac{\pi \Delta}{2}$ the associated maximum supercurrent being^{*)}

$$J_0 = \frac{\pi \Delta}{2e R_n}, \quad (3.6.21)$$

where R_n is the tunneling resistance per unit area of the junction when both metals are in the normal state. For Pb and Sn, the gaps are 1.4 meV and 0.7 meV, leading to $V_{\text{equiv}} (V_{\text{equiv}}/e) \approx 2.2 \text{ meV} (2.2 \text{ mV})$ and 0.7 meV (0.7 mV) respectively. Assuming R_n to be of the order of 1Ω per unit area, implies maximum values of the Josephson supercurrent $J_x = J_0 \sin \delta$ ($\delta = \phi_2 - \phi_1 - \frac{2\pi}{(hc/2e)} \int_1^2 A_x dx$), where A is the vector potential, of the order of $J_0 \approx 1 \text{ mA}$ as experimentally observed.

If is suggestive that the expression (3.6.20) is formally similar to that of the ion-ion potential acting between

^{*)} Tinkham (1975) Ch. 6, Eq. (6-4) and subsequent discussion; see also Anderson (1964) Eq (11) and following discussion.

(198)

two heavy ions in weak contact, namely at a distance a diffusivity away from the grazing distance r_g . In this case the role of the reduced gap is played by a quantity closely related to the reduced radius of curvature^{*)}.

$$U_{aa}^N(r_g+a) \approx -\pi \gamma \frac{R_a R_a}{R_a + R_A} a, \quad (3.6.22)$$

In the above expression $\gamma \approx 1 \text{ MeV/fm}^2$ is the surface tension, $a = 0.63 \text{ fm}$ the diffusivity of the potential, $R_i (= 1.233 A^{1/3} - 0.98 A^{-1/3}) \text{ fm}$ being the radii of nuclei $i = a, A$.

For two identical nuclei $U_{aa}^N(r_g+a) \approx -\pi \gamma R_{aa} a$ which, for for ^{120}Sn has the value $U_{aa}^N(13.43 \text{ fm}) \approx -6 \text{ MeV}$.

Nuclei being leptodermous systems can be described at first, concerning a number of properties, with the help of the liquid drop. Because at the grazing distance the two leptodermous objects overlap, although weakly, two "unit" areas disappear. To reconstruct them one has to separate the two nuclei until these areas are reconstructed again. The energy needed to do so has to compensate the value (3.6.22) namely, in the present case it is 6 MeV.

^{*)} footnote, (4)-(4) from p. (3) handwritten

Microscopically, the interaction (198c) (3)
 (3.6.22) arises from a kind of, weak,
 covalent mechanism. The single-particle
 orbitals of the two individual nuclei
 a and A , are shared when in contact,
 leading to a common mean field,

Similarly, the weak link (3.6.20)
 between the two superconductors, 1
 and 2, is associated with the situation in
 in which each partner of a Cooper pair is
 in a different superconductor. A kind
 of covalent phenomenon, in which
 each Cooper pair is simultaneously
 shared by the two superconductors.

(A)

to p. 198

(4) *) Broglia and Wüther (2005) p. 114 Eq(40),

$$U_{aa}^N(r) = -V_0 / (1 + \exp(\frac{r-R}{a})), \quad V_0 = 16\pi\sigma R_{AAA},$$

$R = R_a + R_A$, which for two ^{120}Sn nuclei leads
 to $R \approx 11.8 \text{ fm}$. For energies somewhat above
 the Coulomb barrier, the grazing distance
 (Eq. (25) p. 128) is $r_g = r_B - \delta \approx 12.3 \text{ fm}$
 $(r_B \approx 13.3 \text{ fm}, \delta \approx 0.5 \text{ fm})$. Thus $(1 + \exp(\frac{r_g+a-R}{a}))$
 ≈ 14.3 .

(4) top (2) footnote

3.7. PHASE COHERENCE

The situation is very different in the case of the wavefunction

$$\begin{aligned} |BCS(\phi)\rangle_{\mathcal{K}} &= \prod_{\nu>0} (U_\nu + V_\nu a_\nu^\dagger a_\nu^\dagger) |0\rangle, \\ &= \prod_{\nu>0} (U_\nu + e^{2i\phi} V_\nu a_\nu'^\dagger a_\nu'^\dagger) |0\rangle, \\ &= \prod_{\nu>0} (U'_\nu + V'_\nu a_\nu'^\dagger a_\nu'^\dagger) |0\rangle, \\ &= |BCS(\phi=0)\rangle_{\mathcal{K}'}, \end{aligned}$$

where

$$U_\nu = |U_\nu| = U'_\nu; \quad V_\nu = e^{2i\phi} V'_\nu (V'_\nu = |V_\nu|),$$

and

$$|BCS(\phi)\rangle_{\mathcal{K}} = \left(\prod_{\nu>0} U_\nu \right) \sum_{n=0,1,2}^{N_0/2} e^{i2n\phi} \left(\sum_{\nu>0} \frac{c_\nu}{\sqrt{n}} P_\nu'^\dagger \right)^n |0\rangle,$$

with

$$c_\nu = \frac{V_\nu}{U_\nu}; \quad n : \# \text{ of pairs}; \quad P_\nu'^\dagger = a_\nu'^\dagger a_\nu'^\dagger,$$

is a wavepacket in particle number,

$$\begin{aligned} |BCS(\phi)\rangle_{\mathcal{K}} &= \left(\prod_{\nu>0} U_\nu \right) \sum_n e^{i2n\phi} |2n\rangle, \\ &= \left(\prod_{\nu>0} U_\nu \right) \sum_n e^{i2n\phi} |N\rangle. \end{aligned} \tag{3.7.1}$$

Let us now apply the gauge angle operator

$$\begin{aligned} \hat{\phi}|BCS(\phi)\rangle_{\mathcal{K}} &= i \frac{\partial}{\partial N} |BCS(\phi)\rangle_{\mathcal{K}} \\ &= \hat{\phi} \left(\prod_{\nu>0} U_\nu \right) \sum_n e^{i2n\phi} |N\rangle = \hat{\phi}|BCS(\phi)\rangle_{\mathcal{K}}. \end{aligned}$$

Thus the state $|BCS(\phi=0)\rangle_{\mathcal{K}'}$ is rigidly aligned in gauge space in which it defines a privileged orientation (z').

An isolated nucleus will not remain long in this product type state. Due to the term $(G/4) \left(\sum_{\nu>0} (U_\nu^2 + V_\nu^2) (\Gamma_\nu^\dagger - \Gamma_\nu) \right)^2$ in the residual quasiparticle Hamiltonian it will fluctuate (QM, ZPF Goldstone mode) it will decay into a state

$$|N\rangle \sim \int d\phi e^{iN\phi} |BCS(\phi)\rangle_{\mathcal{K}}, \tag{3.7.2}$$

question
of phase
 $e^{-2i\phi}$
in eq. (2.47)

member of a pairing rotational band around neutron mass number N : for example the ground states of the Sn-isotopes around $N_0 = 68$ (see Fig. 2.1.3). Because $E_R = (\hbar^2/2I)(N - N_0)^2 = (G/4)(N - N_0)^2 = G/4(\frac{1}{\delta\phi})^2$ is the kinetic energy of rotation in (nuclear) gauge space, and $G/4 \approx 25/(4N_0) \approx 0.0092$ MeV, the wavepacket (3.7.1) will decay³⁵ in the state (3.7.2) in a time of the order of $\hbar/E_R \approx \hbar/(4 \times 0.0092 \text{ MeV}) (N = N_0 \pm 2) \approx 10^{-19} \text{ sec}$. In other words, superfluid nuclei cannot be prepared, in isolation, in states with coherent superposition of different N -values. The common assumption that N is fixed, ϕ meaningless is correct. This is also the case for real superconductors. In fact, the corresponding state (3.7.1) even if prepared in isolation would dissipate because there is actually a term in the energy of the superconductor depending on N , namely the electrostatic energy $e(N - N_0)^2/2C = e^2/2C(\partial/\partial\phi)^2$, where C is the electrostatic capacity. The system will dissipate, no matter how small $\delta\phi$ is. In fact, let us assume $\delta\phi = 1$ degree ($= \pi/180 = 0.017$). The kinetic energy of rotation in gauge space is $\sim (e^2/2C)(1/\delta)^2(\delta N\delta\phi/2\pi \sim 1)$, and

$$\Delta E = \frac{1.44 \text{ fm MeV}}{1 \text{ cm } (1^\circ)^2} \sim 1.44 \times 10^{-13} \text{ MeV}, \quad (3.7.3)$$

which corresponds to an interval of time

$$\Delta t \approx \frac{\hbar}{1 \text{ MeV}} \frac{10^{13}}{1.44} \approx \frac{0.667 \times 10^{-21} \text{ sec}}{1.44} \times 10^{13} \approx 10^{-9} \text{ sec}. \quad (3.7.4)$$

The opposite situation is that of the case in which one considers different parts of the same superconductor. In this case one can define relative variables $n = N_1 - N_2$ and $\phi = \phi_1 - \phi_2$ and again $n = -i\partial/\partial\phi$ and $\phi = i\partial/\partial n$. Thus, locally there is a superposition of different n states: ϕ is fixed so n is uncertain. It is clear that there must be a dividing line between these two behaviors, perfect phase coherence and negligible coherence, namely the Josephson effect.

In the nuclear case, one can view the systems $|BCS(A+2)\rangle$ and $|BCS(A)\rangle$ as parts of a fermion superfluid (superconductor) which, in presence of a proton ($p + (A+2)$) are in weak contact to each other, the $d + |BCS(A+1)\rangle$ system (without scattering, running waves, but as a closed, virtual, channel) acting as the dioxide layer of a Josephson junction (Fig. 3.7.1).

Clearly, again, the total phase of the assembly is not physical. However, the relative phases can be given a meaning when one observes, as one does in e.g.

³⁵ Within this context note that setting in phase at $t = 0$ all the states in which a GDR breaks down through the hierarchy of doorway-states-coupling, they would dissipate like a wavepacket of free particles after 10^{-22} sec (assuming $\Gamma_{GDR} \approx 3 - 4$ MeV). It is of notice that the GDR will eventually branch into the ground state, although $\Gamma_\gamma \ll \Gamma_{GDR}$, in keeping with the fact that the $t = 0$ phase coherent states are individually stationary. What is not stationary is its phase coherence. Pushing the analogy a step further, one can say that in quantum mechanics, while the outcome of an experiment is probabilistic the associated probability evolve in a deterministic way (Born (1926)). This is the reason why a large gamma ray detector will reveal a well defined peak of the resonant dipole state long after its lifetime deadline (\hbar/Γ). Also, while one can obtain a completely (classical) picture of a face making use of single photons, provided one waits long enough.

(See Sect. 1.3)

$$A+2X + p \rightarrow (A_X + t) \rightarrow A+2X + p$$

$(A_X + t) \rightarrow$ i.e.

3.8. HINDSIGHT

201

metallic superconductors, that electrons can pass back and forth through the barrier, leading to the possibility of coherence between states in which the total number of electrons is not fixed *locally*. Under such conditions there is, for instance, a coherence between the state with $N/2$ electrons in one half of the block and $N/2$ in the other, and that with $(N/2) + 2$ on one side and $(N/2) - 2$ on the other.

Under favorable conditions, in particular of Q -value for the different channels involved and, similarly to the so called backwards rise effect, one may, arguably, observe signals of the coherence between systems $(A+2)$ and A in the elastic scattering process $A+2X + p \rightarrow A+2X + p$, $A+2X$ denoting a member of a pairing rotational band (cf. Fig. 3.7.1, see also Fig 2.1.3). It is of notice that the process $A+2X + p \rightarrow A+1X + d \rightarrow A+2X + p$ is likely to be the dominant one concerning the optical potential describing the $A+2X + p$ scattering process. Because $P_2 \approx P_1$, a likely better estimate of $U + iW$ can be obtained taking into account also the transfer back and forth of two nucleons. In keeping with the fact that the sum of the simultaneous and non-orthogonality contributions are much smaller than the successive transfer, only this last process is shown in the NFT-reaction-structure diagram displayed in Fig. 3.7.1.

$A+2X$

ℓ

Whether an effect which may parallel that shown in (c) (backwards rise) can be seen or not depends on a number of factors, but very likely it is expected to be a weak effect. This was also true in the case of the Josephson effect in its varied versions (AC, DC, etc.). In fact, its observation required to take into account the effect of the earth magnetic field, let alone quantal and thermal fluctuations.

3.8 Hindsight

; see also app. 3.B)

This point was not understood by Bardeen who writes "... In my view, virtual pair excitations do not extend across the layer..."; see McDonald (2001); see also Bardeen (1961) and (1962).

The formulation of superconductivity (BCS theory) described by Gor'kov³⁶ allows, among other things for a simple visualization of spatial dependences. In this formulation $F(\mathbf{x}, \mathbf{x}')$ is the amplitude for two Fermions (electrons) at \mathbf{x}, \mathbf{x}' , to belong to the Cooper pair (within the framework of nuclear physics cf. e.g. Fig. 2.6.3 $\Psi_0(\mathbf{r}_1, \mathbf{r}_2)$). The phase of F is closely related to the angular orientation of the spin variable in Anderson's quasiparticle formulation of BCS theory³⁷. The gap function $\Delta(x)$ is given by $V(\mathbf{x})F(\mathbf{x}, \mathbf{x})$ where $V(\mathbf{x})$ is the local two-body interaction at the point \mathbf{x} . In the insulating barrier between the two superconductors of a Josephson junction, $V(\mathbf{x})$ is zero and thus $\Delta(x)$ is also zero.

The crucial point is that vanishing $\Delta(x)$ does not imply vanishing F , provided, of course, that one has within the insulating barrier, a non-zero particle (electron) density, resulting from the overlap of densities from right (R) and left (L) superconductors. Now, these barriers are such that they allow for one-electron-tunneling with a probability of the order of 10^{-10} and, consequently, the above requirement is

³⁶ Gor'kov, L.P. (1959).

³⁷ Anderson (1958); within the framework of nuclear physics cf. e.g. Bohr and Ulfbeck (1988), Potel, G. et al. (2013b) and references therein.

(1958) ←

see ref. p. 248

*

↓ continuity condition

fulfilled³⁸. Nonetheless, conventional (normal) simultaneous pair transfer, with a probability of $(10^{-10})^2$ will not be observed. But because one electron at a time can tunnel profiting of the small, but finite electron density within the layer, $F(x, x')$ can have large amplitude for electrons, on each side of the barrier (i.e. L and R), separated by distances $|x - x'|$ up to the coherence length. Hence, for barriers thick to only allow for essentially the tunneling of one electron at a time, but thin compared with the coherence length, two electrons on opposite sides of the barrier can still be correlated and the pair current can be consistent. An evaluation of its value shows that, at zero temperature, the pair current is equal to the single particle current at an equivalent voltage³⁹ $\pi\Delta/2e$.

The translation of the above parlance to the language of nuclear physics has to come to terms with the basic fact that nuclei are self-bound, finite many-body systems in which the surface, as well as space quantization, play a very important role both as a static element of confinement, as well as a dynamic source for renormalization effects^{40,41}. Under the influence of the average potential which can be viewed as very strong external field ($|V_0| \approx 50$ MeV), Cooper pairs ($|E_{corr}| \approx 1.5$ MeV; see Fig. 2.5.1) will become constrained within its boundaries with some amount of spill out. In the case of the single open shell superfluid nucleus ^{120}Sn , the boundary can be characterized by the radius $R_0 \approx 6$ fm ($\ll \xi \approx 30$ fm), the spill out being connected with the diffusivity $a \approx 0.65$ fm.

Let us now consider a two nucleon transfer reaction in the collision $\text{Sn}+\text{Sn}$ assuming a distance of closest approach of ≈ 14 fm, in which the two nuclear surfaces are separated by ≈ 2 fm (Fig 3.4.1). In keeping with the fact that this distance is about $3 \times a$, the heavy ion system will display a few percent (of saturation) density overlap in the interacting region. Ever so small this overlap of the nuclear surfaces, and so narrow the hole between the two leptodermic systems resulting from it, Cooper pairs can now extend over the two volumes, in a similar way as electron Cooper pairs could be partially found in the R and L superconductors in a Josephson junction. If this is the case, Cooper pair partners can be at distance as large as 26 fm, of the same order of magnitude of the correlation length. In other words, in the reaction $\text{Sn}+\text{Sn} \rightarrow \text{Sn(gs)}+\text{Sn(gs)}$ one expects (mainly successive) Cooper pair transfer of two neutrons which are away from each other by tens of

et al (1995)

³⁸Pippard (2012) see also McDonald (2001).

³⁹In the case of Pb at low temperatures (< 7.19 K (0.62 meV)) this voltage is $\approx 1 \text{ meV}/e = 1 \text{ mV}$ (Ambegaokar and Baratoff (1963); McDonald (2001); Tinkham (1996)).

⁴⁰Within this context it is of notice that the liquid drop model is a very successful nuclear model, able to accurately describe not only large amplitude motion (fission, exotic decay, low-lying collective density and surface vibrations, cf. e.g. Bohr and Wheeler (1939), Barranco, F. et al. (1990), Bertsch (1988), see also Brink, D. and Broglia (2005) and references therein), but also the masses of nuclides (cf. e.g. Moller and Nix), provided the superfluid inertia and shell corrections respectively, are properly considered. Thus, it is an open question whether in the quest of developing more predictive theoretical tools of the global nuclear properties one should develop ever more "accurate" zero range (Skyrme-like) forces, or deal with the long wavelength, renormalization effects and induced interaction.

⁴¹Broglia, R. A. (2002).

1 mA

barrier
 $R \approx 152$

$R V = I$

P. Moller et al. Atom. Data Nucl. Data Tabl. 59, 185-381
(1995)

low energy

fm.

An example of the fact that Cooper pairs will “expand” if the external mean field is weakened, is provided by ^{11}Li in which case, profiting of the weak binding (≈ 380 keV), the extension of the constrained Cooper pair ($\approx 4.58 \text{ fm} \pm 0.13 \text{ fm}$) is similar to that expected in a nucleus of mass number $A \approx 60$, assuming a standard radial behavior, i.e. $r_0 A^{1/3} \text{ fm}$. In keeping with this scenario, it could be expected that moving from one neutron pair addition 0^+ mode of the $N = 6$ isotones^{*} to another one ($|^{11}\text{Li(gs)}\rangle$, $|^{12}\text{Be(gs)}\rangle$ and $|^{12}\text{Be}(0^{++}; 2.24 \text{ MeV})\rangle$) one would see the system expanding, contracting and expanding again, respectively, in keeping with the fact that the external (mean) field is weak, strong, weak respectively, as testified by S_{2n} (380 keV, 3672 keV, 1432 keV). Within this context, the dipole resonance built on top of them is expected to vary in energy from very low ($< 1 \text{ MeV}$) to high (2.71 MeV) to low (0.460 MeV), that is from a symbiotic, to an independent, and, likely, to a (quasi) symbiotic role again. Within this context, in Fig. 3.8.1 an overall view of the pairing vibrational modes associated with $N = 6$ parity inverted closed shell isotones, together with low-energy $E1$ -strength modes is given. The possible candidates to the role of neutron halo pair addition modes and symbiotic state are explicitly indicated (boxed levels).

In Fig. 3.8.2 the $^{11}\text{Li(gs)}$, $^{12}\text{Be(gs)}$ and $\text{Be}(0^{++}; 2.25 \text{ MeV})$ wavefunctions and $|\Psi_0(\mathbf{r}_1, \mathbf{r}_2)|^2$ probability distribution of one Cooper pair partner with respect to the other located at a fixed distance from the CM of the nucleus under study are shown (see also Fig. 2.6.3 (II)). While the results associated with the two ground states have been tested in connection with the experimental findings (Barranco, F. et al. (2001); Rotel et al. (2010, 2014); Gori et al. (2004)), much less is known regarding the accuracy of the predictions associated with $^{12}\text{Be}(0^{++})$.

strength (pygmy resonance)

found

Appendix 3.A Medium polarization effects and pairing

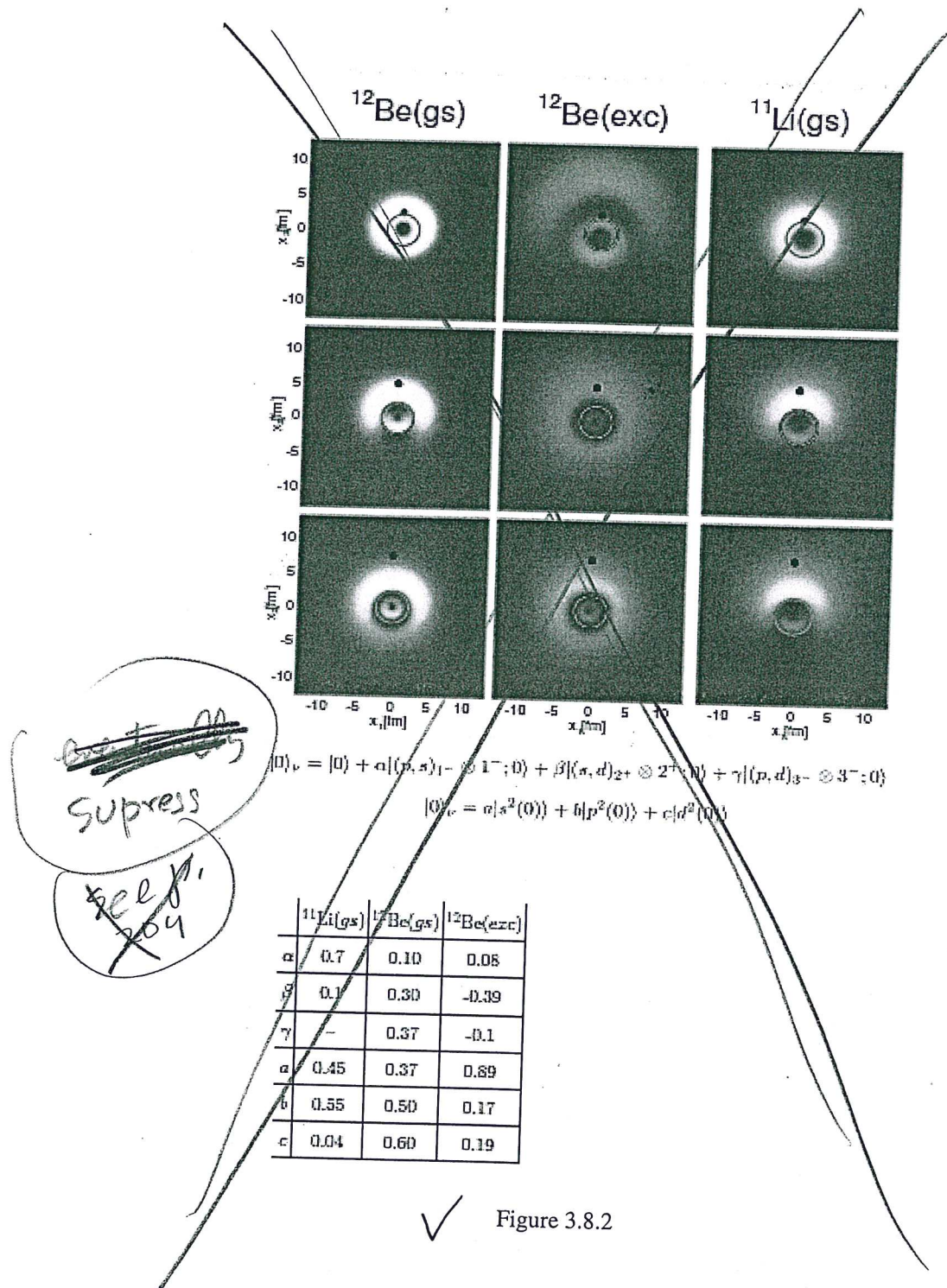
3.A.1 Nuclei

Polarization contributions to the bare nucleon-nucleon pairing interaction through elementary modes of excitation

Elementary modes of excitation constitute a basis of states in which correlations, as found in observables, play an important role. As a consequence, it allows for an economic solution of the nuclear many-body problem of structure and reaction. A first step in this quest is to eliminate the non-orthogonality associated with single-particle motion in different nuclei (target and projectile (*reaction*)). Also between single-particle degrees of freedom and collective modes (vibrations and rotations (*structure*)) typical of an overcomplete, Pauli principle violating, basis. This can be done by diagonalizing, making use of the rules of nuclear field theory (NFT), the particle-vibration coupling (PVC), and the v_{np} (v : four point vertex, bare $NN-$) interaction. In this way one obtains quantities (energies, transition probabilities, absolute value of reaction cross sections) which can be directly compared

*) See e.g., Gori et al (2004) and refs. therein.

generally take out



with the experimental findings. Such a protocol can be carried out, in most cases, within the framework of perturbation theory. For example, second order perturbation theory, in both reaction and structure, as exemplified in Fig. 1.9.3 displaying a NFT (r+s) graphical representation of contributions to the $^{11}\text{Li}(p, t)^9\text{Li}(\text{gs})$ and $^{11}\text{Li}(p, t)^9\text{Li}(1/2^-; 2.69 \text{ MeV})$ processes (see also Fig. 6.1.3). As a result, single-particle states move in a gas of vibrational quanta and become clothed by coupling to them. The quanta couple, in turn, to doorway states which renormalize their properties through self-energy and vertex corrections. Similar couplings renormalize the bare NN -interaction in the different channels. In particular in the 1S_0 (pairing) channel.

Also as a result of their interweaving, the variety of elementary modes of excitation may break in a number of states, eventually acquiring a lifetime and, within a coarse grain approximation, a damping width (imaginary component of the self energy). Moving into the continuum, as for example in the case of direct reactions, one such component is the imaginary part of the optical potential operating in the particular channel selected. It can be calculated microscopically using similar techniques and elements as e.g. those used in the calculation of the damping width of giant resonances. With the help of dispersion relations, the real part of the optical potential can be obtained from the knowledge of the energy dependence of the absorptive potential. In this way, the consistency circle structure-reaction based on elementary modes and codified by NFT could be closed. The rich variety of emergent properties found along the way eventually acquiring a conspicuous level of physical validation. In the case of halo exotic nuclei, in particular in the case of ^{11}Li (bootstrap, Van der Waals Cooper binding, halo pair addition mode (symbiosis of pairing vibration and pigmy) being few of the associated emergent properties) one is rather close to his goal. At that time it would be possible, arguably if there is one, to posit that the *ultima ratio* of structure and reactions, in any case that is associated with pairing and Cooper pair transfer in nuclei, have been unveiled⁴².

Effective moments

At the basis of the coupling between elementary modes of excitation, for example of single-particle motion and of collective vibrations, is the fact that, in describing the nuclear structure it is necessary to make reference to both (all) of them simultaneously and in an unified way.

Within the harmonic approximation the above statement is economically embodied in e.g. the relation existing between the collective ($\hat{\alpha}$) and the single-

⁴² In the above paragraph we allow ourselves to paraphrase Jacques Monod writing in connection with biology and life: *L'ultima ratio de toutes les structures et performances téléonomiques des êtres vivants est donc enfermée dans les séquences des radicaux des fibres polypeptidiques "embryons" de ces démons de Maxwell biologiques que sont les protéines globulaires. En un sens, très réel, c'est à ce niveau d'organisation chimique qui gît, s'il y en a un, le secret de la vie. Et saurait-on non seulement décrire les séquences, mais énoncer la loi d'assemblage à laquelle obéissent, on pourrait dire que le secret est percé, l'ultima ratio découverte* (J. Monod, *Le hasard et la nécessité*, Editions du Seuil, Paris, 1970).

Monod (1970),

bring to refs

to be compared with the empirical value

$$\Delta \approx 1.4 \text{ MeV} \quad (3.A.31)$$

of superfluid medium heavy mass nuclei like ^{120}Sn .

While the relations (3.A.28) can hardly be relied to provide a quantitative number, they testify to the fact that induced pairing is expected to play an important role in nuclei. These expectations have been confirmed by detailed confrontation of theory and experiment⁴⁹.

Hindsight

Static polarization effects can be important in clothing single-particle states. For example, effective charges and induced interactions associated with moments induced by giant resonances⁵⁰. However, retarded ω -dependent self-energy effects and induced interactions are essential in describing structure and reactions of many-body systems. Examples are provided by the bootstrap binding of the halo neutrons (pair addition mode) to ^9Li , leading to the fragile $|^{11}\text{Li}(gs)\rangle$, displaying a $S_{2n} \approx 0.380$ MeV as compared to typical values of $S_{2n} \approx 18$ MeV as far as structure goes, and by the $^1\text{H}(^{11}\text{Li}, ^9\text{Li}(1/2^-; 2.69 \text{ MeV}))^3\text{H}$ population of the lowest member of the $(2^+ \times p_{3/2}(\pi))_J$ -multiplet of ^9Li , as far as reaction goes. If there was need for support coming from other fields of research, one can mention just two: van der Waals force and superconductivity.

It was recognized early in the study of dipole-dipole interaction in atomic systems that, of the variety of contributions to the van der Waals interaction, the retarded, fully quantal contribution, arising from (dipole) zero point fluctuations (ZPF) of the two interacting atoms or molecules, and the only active ~~also~~^{it} in the case of non-polar molecules⁵¹, play an overwhelming role, static-induced interactions being less important (App. 2.D). A consequence of this result is the fact that the limiting size of globular proteins (≈ 50 Å) is controlled by the strong damping undergone by the retarded contribution to the amino acid interaction, when the frequency associated with the back and forth propagation of the force matches the molecules electronic frequencies⁵².

⁴⁹ See e.g. Idini et al. (2015).

⁵⁰ See e.g. Bohr, A. and Mottelson (1975), Eqs. (6-217) and (6-228).

⁵¹ Within this context van der Waals and gravitation are two forces which are universally operative, acting among all bodies.

⁵² It is of notice that similar arguments (cf. Sect. 2.6) are at the basis of the estimate (2.6.5) concerning the size of the halo nucleus ^{11}Li , a quantity which is influenced to a large extent by the maximum distance (correlation length) over which partners of a Cooper pair are virtually (~~it~~ materializes only if particle, normal, density allows for) but solidly anchored to each other (localized), and have to be seen as an (extended) bosonic entity and not as two fermions. The fact that Cooper pair transfer proceeds mainly in terms of successive transfer controlled by the single-particle mean field, reinforces the above physical picture of nuclear pairing. Even under the effect of extremely large, as compared to the pair correlation energy, external single-particle fields, namely that of target and projectile, the Cooper pair field extends over the two nuclei, permeating the whole summed nuclear volume also through a tiny density overlap⁵³.

with a cross section
 $\sigma(3/2^- \rightarrow 1/2^-; 2.69 \text{ MeV}) \approx 1 \text{ mb}$

interaction, interaction
which in the case of low
temperature superconductors
leads

Concerning superconductivity, the overscreening effect which binds weakly Cooper pairs stems from a delicate ω -dependent phenomenon leading, eventually, to one of the first macroscopic manifestations of quantum mechanics, as e.g. "permanent" magnetic fields associated with supercurrents.

The statement "*Life at the edge of chaos*" coined in connection with the study of emergent properties in biological molecules (e.g. protein evolution, folding and stability) reflects the idea, as expressed by de Gennes⁵³, that truly important new properties and results can emerge in systems lying at the border between rigid order and randomness, as testified by the marginal stability and conspicuous fluctuations characterizing, for example, nuclear Cooper pairs at the dripline and in metals, and that of proteins of e.g. viral particles like the HIV-1- and HCV-proteases⁵⁴.

Let us conclude this short comment, quoting again de Gennes but doing so with the hindsight of twenty years of nuclear research which have elapsed since "Les objets fragiles" was first published. The chapter entitled "Savoir s'arrêter, savoir changer" starting at p. 180 opens with the statement "En ce moment, la physique nucléaire (la science des noyaux atomiques) est une science qui, à mon avis, se trouve en fin de parcours... C'est une physique qui demande des moyens coûteux, et qui s'est constituée par ailleurs en un puissant lobby. Mais elle me semble naturellement exténuée... je suis tenté de dire: "Arrêtons"... mais ce serait aussi absurde que de vouloir arrêter un train à grande vitesse. Le mieux serait d'aiguiller ce train sur une autre voie, plus nouvelle et plus utile à la collectivité."

In a way, and even without knowing de Gennes remark, part of the nuclear physics community have followed it, capitalizing on the novel embodiment that concepts like elementary modes of excitation, spontaneous symmetry breaking and phase transitions have had in this paradigm of finite many-body (FMB) system the nucleus represents, where fluctuations, as a rule, dominate over potential energy effects. The use of these concepts tainted by FMB system effects as applied to proteins, in particular to the understanding of protein folding may, arguably shed light on the possibility of designing leads to drugs which are less prone to create resistance⁵⁵.

3.A.2 Metals

Plasmons and phonons (jellium model)

The expression of the electron plasmon frequency of the antenna-like oscillations of the free, conduction electrons of mass m_e and charge $-e$, against the positive charged background (jellium model) is

$$\omega_{ep}^2 = \frac{4\pi n_e e^2}{m_e} = \frac{3e^2}{m_e r_s^2}, \quad (3.A.32)$$

⁵³de Gennes (1994).

⁵⁴See e.g. Broglia, R. A. (2013).

⁵⁵See e.g. Broglia, R. A. (2013) and refs. therein.

(2005)
↑
Nuovo Cimento

where

$$n_e = \frac{3}{4\pi} \frac{1}{r_s^3}, \quad (3.A.33)$$

are the number of electrons per unit volume, r_s being the radius of a sphere whose volume is equal to the volume per conduction electron,

$$r_s = \left(\frac{3}{4\pi n_e} \right)^{1/3}, \quad (3.A.34)$$

that is, the radius of the Wigner-Seitz cell.

For metallic Li⁵⁶

$$n_e = 4.70 \frac{10^{22}}{\text{cm}^3} = \frac{4 \times 10^{-2}}{\text{\AA}^3}, \quad (3.A.35)$$

while

$$r_s = \left(\frac{3\text{\AA}^3}{4\pi \times 4.7 \times 10^{-2}} \right)^{1/3} = 1.72\text{\AA}, \quad (3.A.36)$$

implying a value $(r_s/a_0) = 3.25$ in units of Bohr radius ($a_0 = 0.529\text{\AA}$).

Making use of

$$\alpha = 7.2973 \underbrace{\frac{e^2}{\hbar c}}_{\times 10^{-3}} \quad (3.A.37)$$

and

$$e^2 = 14.4 \text{ eV \AA}, \quad (3.A.38)$$

one obtains

$$\hbar c = \frac{14.4 \text{ eV \AA}}{7.2973 \times 10^{-3}} = 1973.3 \text{ eV \AA}. \quad (3.A.39)$$

Making use of the above values and of

$$m_e c^2 = 0.511 \text{ MeV}, \quad (3.A.40)$$

one can write

$$\hbar^2 \omega_{ep}^2 = \frac{(\hbar c)^2}{m_e c^2} \frac{3e^2}{r_s^3} = \frac{(1973.3 \text{ eV \AA})}{0.511 \times 10^6 \text{ eV}} \frac{3 \times 14.4 \text{ eV \AA}}{(1.72 \text{ \AA})^3} = 64.69 \text{ eV}^2 \quad (3.A.41)$$

leading to⁵⁷

$$\hbar \omega_{ep} = 8.04 \text{ eV} \approx 1.94 \times 10^9 \text{ MHz} \quad (3.A.42)$$

For the case of metal clusters of Li, the Mie resonance frequency is

$$\hbar \omega_M = \frac{\hbar \omega_{ep}}{\sqrt{3}} = 4.6 \text{ eV}. \quad (3.A.43)$$

⁵⁶f. page 5, table 1.1 of Ashcroft and Mermin (1987).
⁵⁷Kittel (1996) Table 2, p. 278.